Second-Harmonic Broad-Band 60-200 GHz InP Transferred Electron Device and Oscillators

S.H. Jones, M.F. Zybura*, J.E. Carlstrom[+], T. O'Brien

Applied Electrophysics Laboratory, University of Virginia, Charlottesville, VA
*Litton Solid State, Santa Clara, CA
[+]Department of Astrophysics, University of Chicago, Chicago, Ill

Abstract

Theoretical and experimental analysis of a single-style second-harmonic InP Transferred Electron Oscillator is presented for the 60-200 GHz frequency band. It is experimentally shown that this single device is extremely broad band and produces moderate amounts of second-harmonic output power (8-85 mW) between 170-63 GHz. Four different cavity designs are considered. A continuously tunable cavity is shown to produce 30-40 mW of power over the 120-147.5 GHz range without any detectable frequency jumps or power dips. A combination of High Frequency Structure Simulator, Microwave Design Software, and Drift-Diffusion-Harmonic-Balance analysis is used to fully self-consistently analyze the TEO operation. Simulations are capable of predicting operating frequencies to within several GHz and output powers to within about 20% accuracy.

Introduction

Many high frequency heterodyne receivers for radio astronomy and atmospheric science research require low noise, reliable, and moderate power sources in the 60-200 GHz regime. Presently, many heterodyne receivers in this frequency band are using InP Transferred Electron Devices (TED) as the local oscillator (LO) source. Also, to generate LO power at the higher frequencies above about 110 GHz, Schottky Barrier Varactor frequency multipliers driven by InP Transferred Electron Oscillators (TEO) are commonly used. Most the InP TEDs in use today are NN+ type devices developed and manufactured by Litton Solid State, and are current limiting or Stable Depletion Layer (SDL) devices [1,2]. These devices are similar to conventional N+NN+ Gunn Diodes, but differ in the mode of operation since an NN+ structure with a very low barrier non-ohmic cathode is incorporated [2]. Although researchers have demonstrated excellent results in the 60-200 GHz regime using N+NN+ Gunn diodes [3,4], the SDL NN+ devices are often preferred for their low operating currents(150-250 mA), lower operating temperature, higher efficiency (2-10%), and commercial availability.

In general, second-harmonic TEOs are realized by reactively terminating the large fundamental oscillation, and coupling to the second-harmonic output power resulting from the strong nonlinear conductance and reactance of the device [5]. The advantage of this design is the low noise associated with the high Q of the fundamental oscillation, combined with the easy tuning and minimal load pulling of the second-harmonic output power. However, as described here, the high Q resonator at the fundamental frequency limits the bandwidth of any one oscillator cavity. In this paper we offer experimental results demonstrating that a single InP, SDL mode, second-

harmonic TEO can operate over the very broad band of about 63-170 GHz; the theoretical results indicate that device operation from 60-200 GHz with this single device is very reasonable given proper cavity design. All the results reported here are for moderate power (10-100mW), and second-harmonic TEO operation. The emphasis of this report is to verify both experimentally and theoretically that the intrinsic bandwidth of high frequency, SDL mode, InP TEDs is on the order of 100 GHz; the typically narrow operational-bandwidth that is observed for most TEOs is associated with the high unloaded circuit Q and other cavity properties. Hence, a number of different broad-band and narrow-band cavities had to be used in this investigation in order to achieve good oscillator operation over the entire range of 63-170 GHz. Certainly, to optimize performance over some narrow-band within this 60-200 GHz range both the diode and cavity design should be fully optimized. However, the device described here does perform well over the entire frequency range, and as expected performs particularly well near the center of the band.

Oscillator Properties and Numerical Simulation

Device Properties

The broad-band device investigated here is a 62.5 um diameter NN+ InP current-limiting TED [1]. The N-type active layer is nominally doped to 1×10^{16} cm^{-3} and is about 1.8 um long. An integral heat sink fabrication process is used to reduce thermal resistance, and the N+ substrate region is only 10 um thick to minimize parasitic resistive loss. A very shallow barrier cathode contact serves to restrict current flow and force the SDL mode of operation. Details of the fabrication process, operation, and design for this device are given in references 1,2. The devices are packaged in standard pill-packages incorporating a quartz dielectric-ring to enclose the device. The inner diameter of the quartz ring is nominally 250 um, the outer diameter is about 300 um, and the ring is about 25 um thick. Au preformed-crosses are typically used to bond the InP device anode to the package lid via the quartz dielectric-ring stand-off. For the highest frequency 170 GHz devices, a six-lead preformed-star was used. This bonding configuration is needed to reduce the series inductance to the diode and increase the operating frequency. A schematic of the device is given in Figure 1. The quartz ring package is not shown in the figure; it is bonded to the heatsink and surrounds the diode.

Cavity Properties

Several second-harmonic cavities and bias-choke structures were used to experimentally explore the maximum bandwidth capability of the described device,. The inherent narrow bandwidth of the high Q cavity at the fundamental makes it very difficult to achieve high performance over a broadband (although the device is inherently broad band). Hence, four separate cavities all similar to those described by Carlstrom [5] were used to achieve reasonable power and performance across the entire 64-170 GHz band (using the single-style device described above). A number of different devices

having the same specifications and very similar operating characteristics were used throughout this investigation. Figure 2 shows the basic cavity configuration.
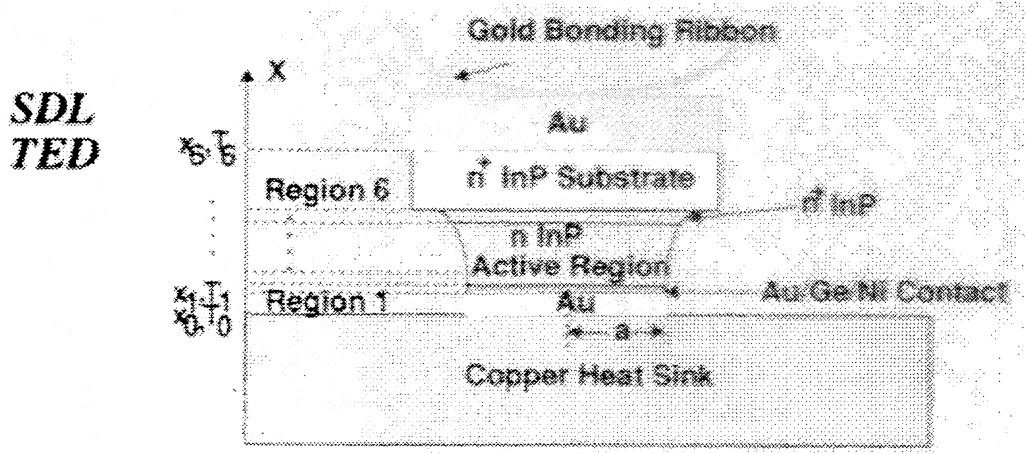

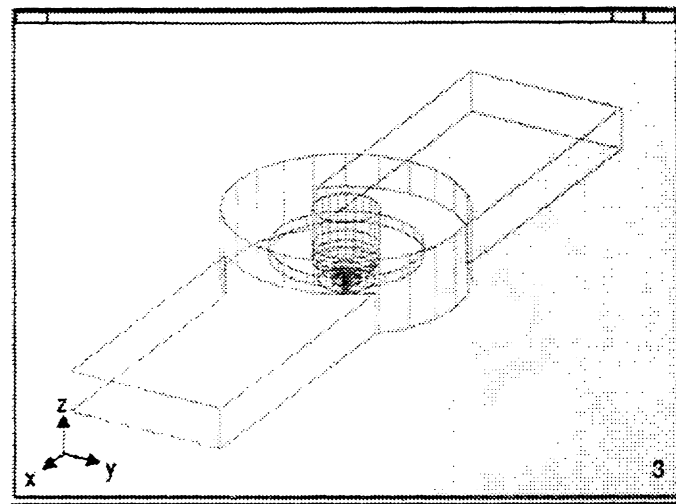**Figure 1   Cross Sectional Schematic of the SDL TED**

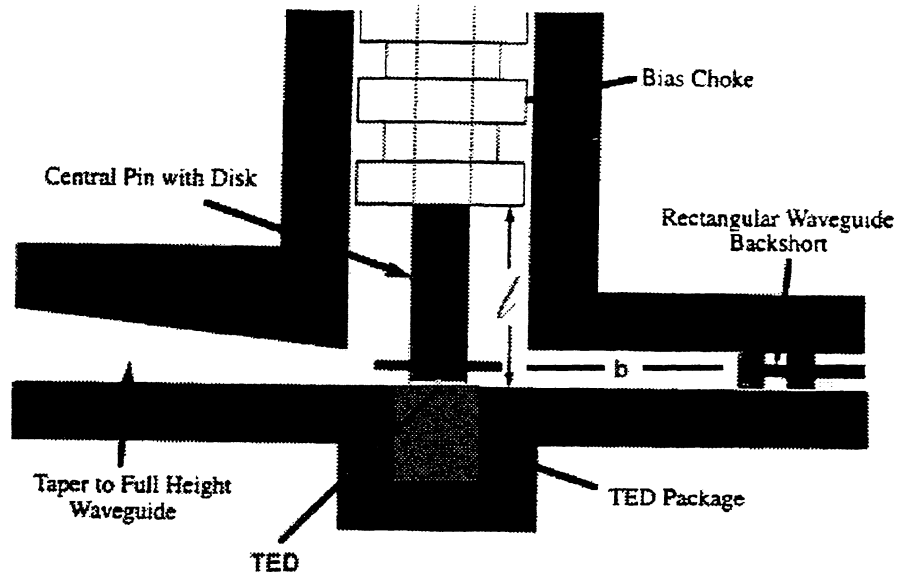**Figure 2   (a) Second-harmonic TEO cavity oblique view**

Figure 2 (b)   Second Harmonic TEO cavity cross sectional view

Broad-band continuously-tunable Carlstrom-style cavities were used for the 94 - 147 GHz (noted wr8-Carl in table 1) as well as the 70-100 GHz band (noted wr10-Carl in table 1). For these cavities the frequency is continuously tunable by mechanically adjusting the height (*l*) of the inner coaxial resonator. This alters the resonant frequency of the fundament tone; as *l* is decreased the frequency is increased. The dimensions of the horizontal waveguide section correspond to wr8 and wr10 waveguide respectively. Also, wr6 and wr10 fixed-frequency cavities were used to investigate select frequencies between 170 and 110 GHz respectively (noted wr10-wr6 and wr6 in table 1). For the fixed-tune cavities the height (*l*) is not adjustable. The power-backshort and output waveguide section in all cases are cutoff at the fundamental operating frequency to insure high Q at the fundamental and minimal load pulling while adjusting the output power. All cavities have adjustable waveguide backshorts to adjust *b*, and control the second-harmonic impedance presented to the diode. This controls the second-harmonic power at the output. Adjustment of *b* only slightly changes the frequency since the fundamental is cutoff in the backshort section and the frequency is predominantly controlled by height (*h*) of the inner coaxial resonator. The wr10-wr6 cavity in Table 1 has wr10 dimensions for the inner cavity and backshort, but a wr10 to wr6 transition at the output to cutoff the fundamental oscillation at the output.

Numerical Simulation

Theoretical investigations of the devices, the cavities, and the devices operating in the cavities were completed using numerical simulation and computer aided design techniques. The properties of the device were explored using unique numerical simulation codes that self-consistently incorporate physical device simulation and harmonic-balance nonlinear circuit simulation [6]. Electron transport and current flow

within the device is achieved by self-consistently solving Poisson's Equations, the 0th and 1st moments of the Boltzmann Transport Equation (current equations) , and the Heat Equation. Since the devices are perfectly cylindrical and relatively large, a one-dimensional finite difference Crank-Nicholson technique is used to solve the set of time and space dependent nonlinear differential equations under large signal excitation. Both electric field dependent and temperature dependent electron mobility and diffusivity are incorporated into the current equations to account for complex transport phenomena under high frequency and large signal operation. The dependence of electron mobility and diffusivity on electric field and temperature was extracted from Monte Carlo analysis of electron transport in the InP material. A unique Accelerated Fixed Point harmonic balance technique [7] is combined with the electron transport analysis to complete the actual oscillator simulation. This combined analysis is referred to as the Drift-Diffusion-Harmonic-Balance analysis (DDHB), and requires detailed knowledge of the circuit embedding impedance as seen by the device. Embedding impedance at the fundamental frequency and at the first six harmonics are inputs to the DDHB code. The other inputs to the DDHB code include device area, cathode barrier height, device doping profile, active layer length, heat sink and substrate parameters, and DC bias. Oscillator characteristics such as power, current and voltage verses time, and device temperature profile are self-consistently and autonomously calculated. Numerical convergence for the DDHB occurs when the Kurokawa conditions for two-terminal oscillators are satisfied (linear circuit embedding impedance is equal-and-opposite to the nonlinear device impedance at all six harmonic frequencies) [8]. Since the DDHB simulations include device, circuit, and thermal analysis, very accurate results for oscillator power and behavior are achievable.

High Frequency Structures Simulator (HFSS) is used to numerically simulate the electromagnetic fields in the cavities at a specific frequency. HFSS is a three dimensional electromagnetic solver that uses finite element techniques to solve Maxwell's equations. Also, using HFSS the exact embedding impedance presented to the device can be calculated for a range of frequencies, backshort positions, pin and disk geometry, and package geometry. For the fixed-tuned wr6 cavity and the wr8-Carl cavity (see Figure 2 and table 1) the entire oscillator structure including the device package has been simulated with HFSS. This allows one to view the internal fields and cavity behavior, and makes it possible to accurately calculate the embedding impedance that is needed for the DDHB simulations. The embedding impedance is calculated by de-embedding and normalizing the S-parameters calculated by HFSS, and then using MDS to calculate the impedance at the position of the diode from the S-parameters. The HFSS probe is a 60 um diameter coaxial probe placed at the precise location of the diode. Correlation between theory and experiment is accurate to within 20% when using the combined analysis techniques of HFSS, MDS, and DDHB [6]. To fully explore the coupled effects of cavity and device properties on the oscillator operation, simulations were completed to calculate the output power as a function of backshort position and cavity geometry. This required several hundred DDHB simulations to be completed and scores of HFSS simulations. To reduce computation time, distributed computing techniques are used for the DDHB code.

Results and Discussion

Theoretical Analysis of Inherent InP Device Properties

Using the DDHB simulator, the small signal negative resistance of the 1.8 um long TED was explored. Simulations were run for fundamental frequencies (f1) ranging from 25-100 GHz (second-harmonic frequencies, f2, between 40-200 GHz). For this analysis the device was driven with a small AC signal (20 mV) at f1 and a DC bias of 8-10 volts. The current and voltage verses time, diode impedance, and power were self-consistently calculated at each operating point, and the first six harmonic tones. The small signal negative resistance of the diode (ReZ_{diode}) at the fundamental frequency ranged from about -10 ohms to -0.7 ohms for 25 GHz to 100 GHz respectively. This corresponds well with the small signal analysis presented in reference 2, and indicates that oscillator operation is predicted over a very broad band. Upon turning on the diode there is a current pulse applied to the high Q resonator, and a subsequent harmonic impulse response. If the resonator center frequency is within the frequency band of negative resistance, the harmonic response near the center frequency will be amplified. As the voltage amplitude of the signal increases, the diode negative resistance decreases (see Figure 3 and 4) until the $ReZ_{diode} = -ReZ_{circuit}$.
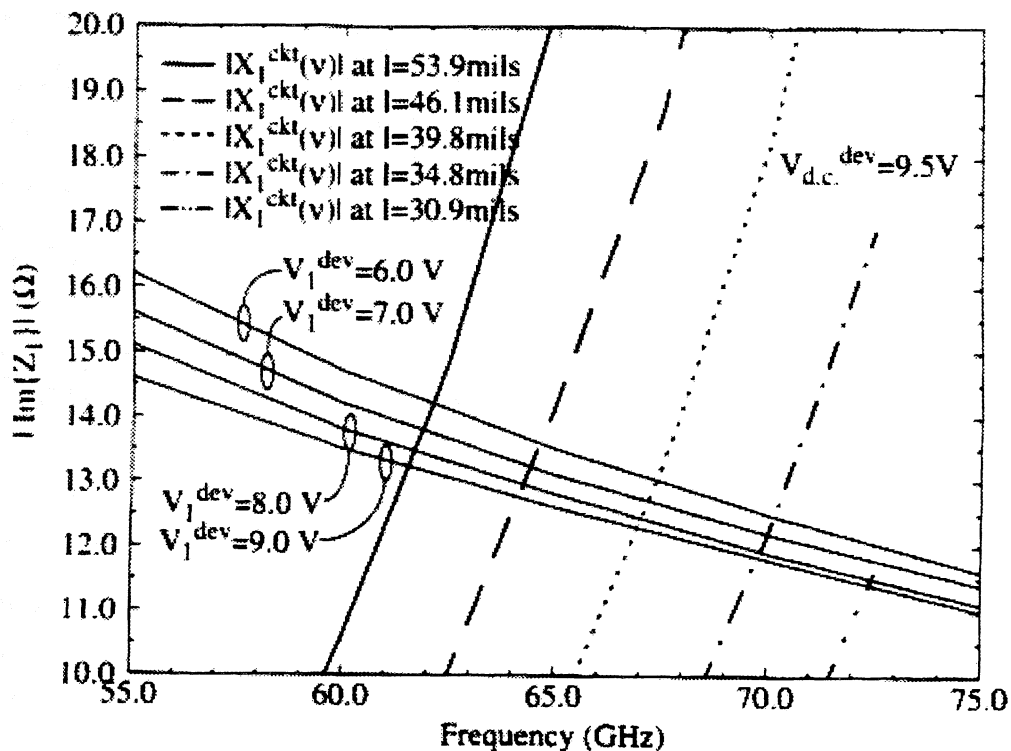

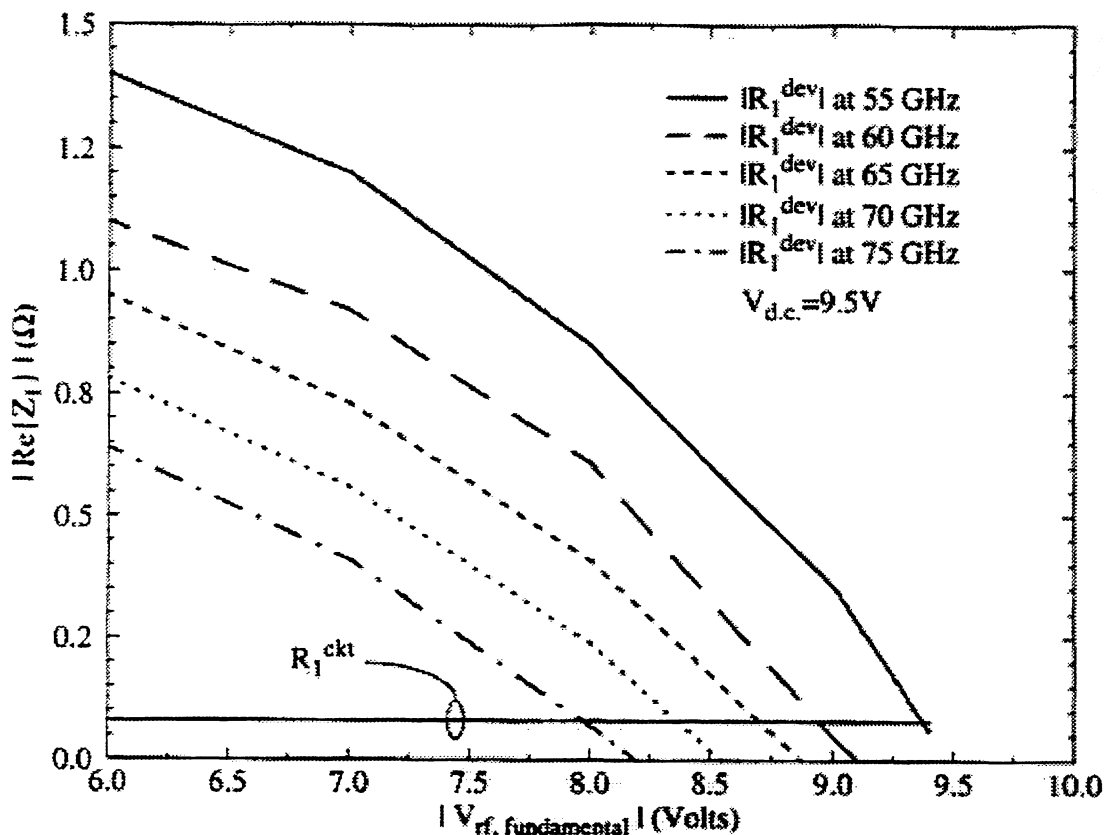
Figure 3 Operating Points as predicted by the DDHB and HFSS simulations

Figure 4   Operating Points as predicted by DDHB and HFSS simulations

The frequency changes until $ImZ_{diode} = -ImZ_{circuit}$, $f1 = 1/(ImZ_{diode} ImZ_{circuit})^{1/2}$, and a stable oscillation is established (Kurokawa condition, [8]). Since the fundamental frequency is reactively terminated, the magnitude of the voltage oscillation increases until $ReZ_{diode} = -R_{parasitic}$, where $R_{parasitic}$ is the parasitic resistance of the device contacts, and the cavity loss. Hence, voltage oscillations will occur if the magnitude of the $ReZ_{circuit} + R_{parasitic}$ is less than the magnitude of ReZ_{diode}. However, as indicated by the Kurokawa condition, stable oscillations are only possible if the condition $ImZ_{diode} = -ImZ_{circuit}$ can be achieved, and the magnitude of the derivative of the diode resistance with respect to the RF voltage, $dReZ_{diode}/dV_{rf}$ at the fundamental is less than one. If this condition is not possible, then the requirement that $ReZ_{diode} = -R_{parasitic}$ is also not possible as the RF voltage increases. Large Signal DDHB simulations were completed over the frequency range of 25-100 GHz (similar to Figure 4) to directly calculate the simplified stability criteria $dReZ_{diode}/dV_{rf} < 1$. At all frequencies over the band and DC biases between 8-10 volts the stability criteria was achieved. These small signal and large signal DDHB simulations therefore predict that stable oscillation is expected over the frequency range of about $f1 = 25-100$ GHz for DC bias between 8-10 volts. Second-

harmonic operation and moderate power is therefore predicted over the frequency range of f2 = 50-200 GHz.

The steady state oscillator behavior was analyzed by simulating the above described device at each frequency in the band, at a DC bias of 10 volts, and a second-harmonic embedding impedance of $Z_{circuit}$ = 7+j7 ohms. Figure 5 shows the theoretical maximum second-harmonic output power verses frequency for this device under these conditions.

Calculated Second Harmonic Power vs. Frequency (DDHB)

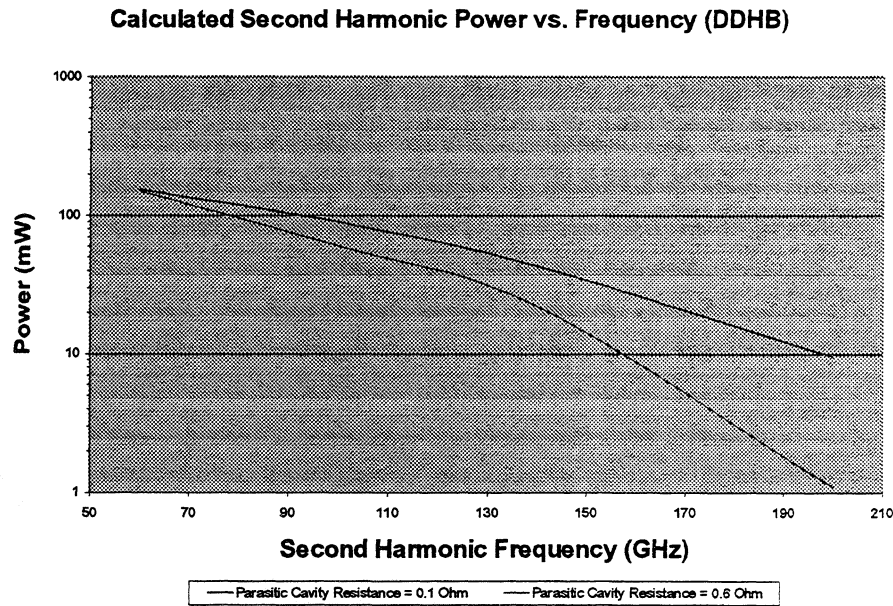| | Parasitic Cavity Resistance = 0.1 Ohm | Parasitic Cavity Resistance = 0.6 Ohm |

Figure 5   Simulated Maximum Second Harmonic Power vs. Frequency

As seen the DDHB simulations predict that this single device can produce 150-10 mW of second-harmonic output power over the entire range of 60-200 GHz if the appropriate embedding impedance is presented to the diode. The effects of $R_{parasitic}$ at the fundamental frequency are also included. At the fundamental frequency ReZ_{diode} = - $R_{parasitic}$ and the ImZ_{diode} ranged from 22-8 ohms for f1 = 30-100 GHz respectively. Since the waveguide is cutoff at the fundamental, the real part of the fundamental circuit impedance is nearly zero ohms. The ReZ_{diode} is essentially equal to the parasitic resistance of the device plus any cavity losses. When the cavity loss increases from 0.1 ohm to 0.6 ohm at f1, there is a significant reduction in the second-harmonic output power. As the real part of the impedance increases at the fundamental, power is internally dissipated in the cavity, and the magnitude of the voltage oscillation is greatly reduced. For negative resistance diode oscillators, the magnitude of the fundamental voltage oscillation is reduced as the square of the real part of the fundamental impedance. This is exactly the case for these diodes as shown in Figure 4. Hence, as the real part of the fundamental embedding impedance increases, the magnitude of fundamental voltage is reduced, and subsequently, the magnitude of the second-harmonic voltage (V_{rf2}) is

119

reduced. Since the power delivered at the second-harmonic frequency (P2) is given by P2 = $V_{rf2}^2/2ReZ_{2diode}$, the output power is reduced for all possible load impedance. Since the small signal negative resistance is smaller at higher frequencies, the increase of $R_{parasitic}$ to 0.6 ohms reduces the second-harmonic output power more severely at higher frequencies. Therefore, these DDHB simulations indicate that 150-10 mW of second-harmonic output power is achievable from a single-style TED provided the fundamental frequency is reactively terminated and the second-harmonic circuit impedance is near 7 + j7 ohms. Although not shown here, 100% variation in the second-harmonic circuit impedance (from 7 +j7 ohms) only produced approximately a 50% variation in the second harmonic output power.

Theoretical Analysis of Inherent Cavity and Oscillator Properties

Although the above analysis indicates that the InP TEDs are inherently very broad band devices, the oscillators are typically narrow band since the cavities are very high Q at the fundamental frequency (low Q at the second-harmonic). Hence, HFSS analysis of the intrinsic cavity properties such as impedance and unloaded Q have been completed. Since the variation in the ImZ_{diode1} with bias voltage is relatively small, only 100-300 MHz of bias frequency-tuning is typically possible with these devices. Varactor tuning the $ImZ_{circuit1}$ and subsequently frequency tuning is possible for very narrow bands, but reduces the oscillator performance by introduce parasitic loss into the high Q fundamental resonator. Therefore, mechanically adjusting the coaxial resonator height (*l*) is the only practical technique for broad band frequency tuning. As described below, the wr8-Carl cavity demonstrated the largest continuous tuning bandwidth of the four cavities investigated. Therefore, extensive HFSS simulations were completed for this cavity. The cavity was analyzed for different coaxial resonator heights (*l* in Figure 2), and corresponding fundamental frequency ranges from 49-72 GHz, second-harmonic frequencies ranging from 99-145 GHz, and appropriate third harmonic frequencies. HFSS was used to visual the electromagnetic fields for different cavity configurations and at different frequencies. Also, using a combination of HFSS and Microwave Design Software (MDS) the circuit impedance seen by the diode was directly calculated. Figure 2b illustrates how the entire cavity and device package was carefully drawn and incorporated into the HFSS analysis.

Figures 6 and 7 show snapshots of the time varying electric field in the wr8-Carl cavity 140 and 108 GHz respectively. The plot for f2 = 140 GHz corresponds to the precise dimensions of the wr8-Carl cavity that was used to experimentally measure about 40 mW of output power at 140 GHz. Although not shown, at 70 GHz the fields are confined to the coaxial resonator within the center of the cavity. Although not illustrated here, the time variation of the electric field at 70 GHz is a TEM oscillation driven by the diode and disc region.. As expected, the 140 GHz oscillation is coupled to the output and power is delivered to the load. The disk serves as transformer to reduce the load impedance as seen by the diode. The cavity was simulated at the fundamental, second-harmonic, and third-harmonic frequency for coaxial resonator heights corresponding to observed second-harmonic output power at 99, 100, 108, 116, 119, 120, 125, 130, 140,

and 145 GHz. Operation at all these frequencies with the exception of f2 = 108 GHz is very similar to that shown in Figure 6..

At f2 = 108 GHz a strong resonance occurs between the disc and the upper coaxial section that shorts-out the diode at the second harmonic. Figure 7 shows the relatively weak second-harmonic fields being shorted between the disc and the coaxial wall. This essentially demonstrates the phenomena of a power dip in the broad band operation of the TEO. The second-harmonic oscillator is well behaved over most the 99-145 GHz band as *l* is decreased until the severe resonance condition at the second-harmonic occurs near 108 GHz.
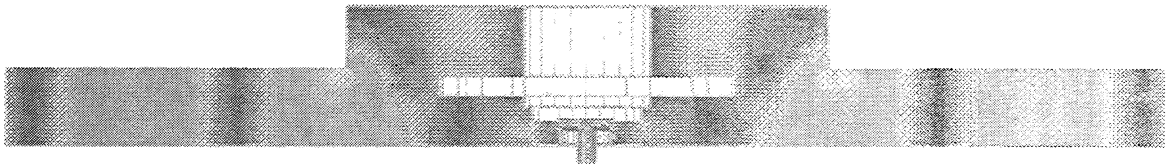

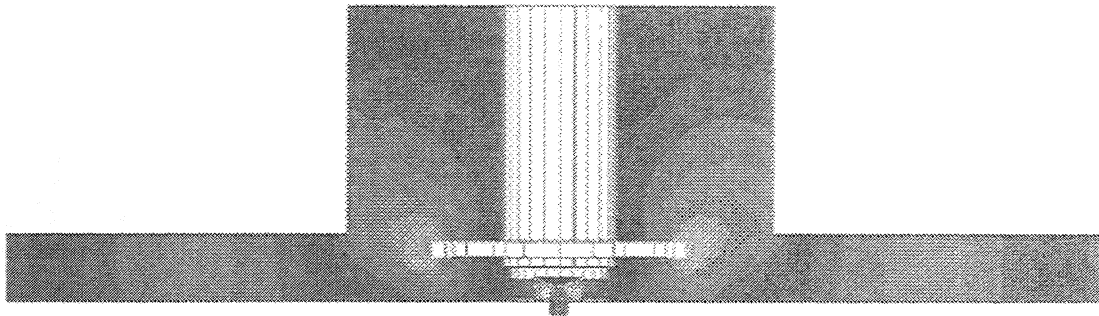**Figure 6   HFSS simulation of the wr8-Carl cavity at 140 GHz**

Figure 7   HFSS simulation of wr8-Carl cavity at 108 GHz

To further illustrate the effects of cavity geometry on the device embedding impedance, HFSS and MDS were used to directly calculate the embedding impedance at many frequencies between 99-145 GHz (second-harmonic), and 49.5-72.5 GHz (fundamental). Also, the impedance at each frequency verses the position of the power backshort was calculated. Figures 8, 9 show the calculated circuit impedance seen by the diode at 70, 140, and 108 GHz as a function of the power backshort position (varying *b* in Figure 2).
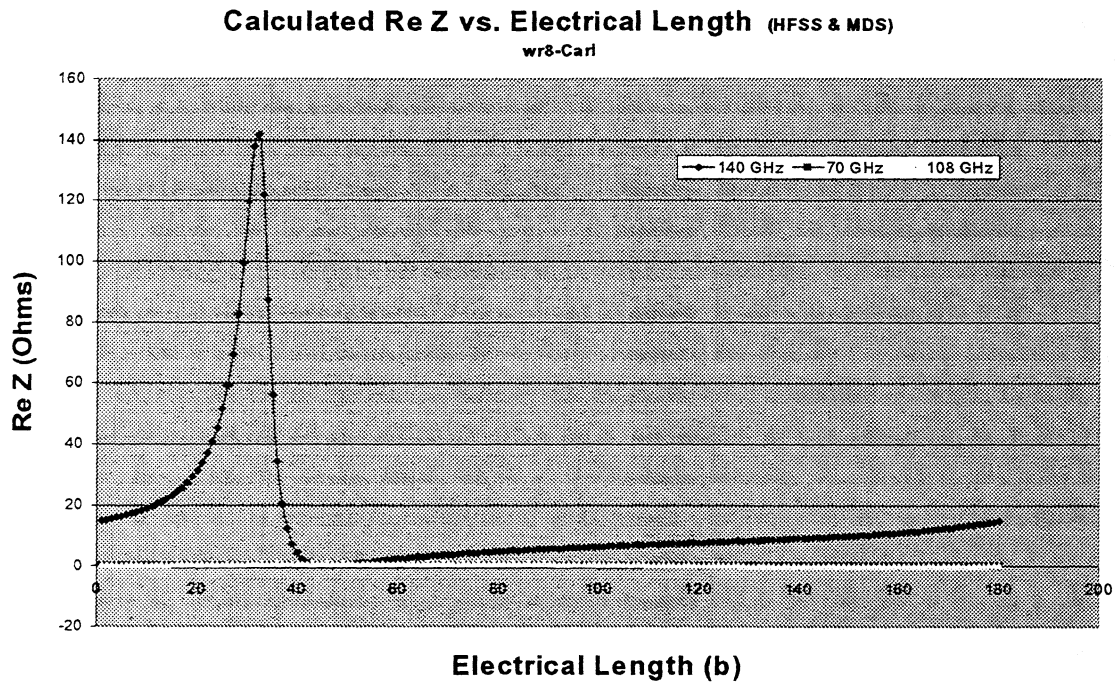
Calculated Re Z vs. Electrical Length (HFSS & MDS)
wr8-Carl

Figure 8   Re Z as a function of backshort position

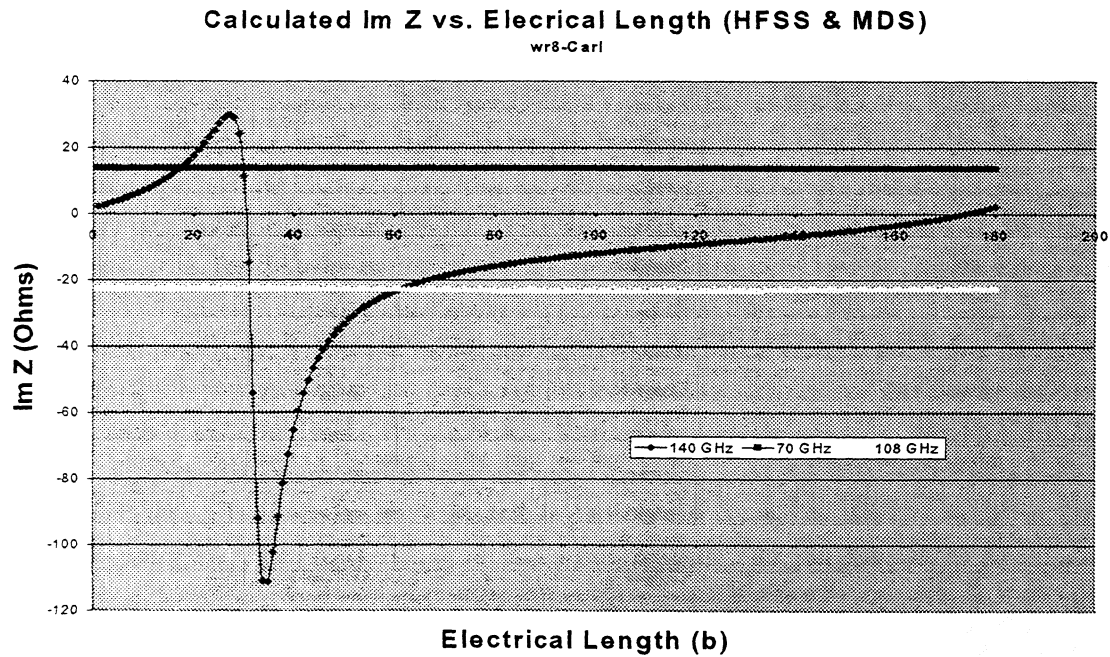**Calculated Im Z vs. Elecrical Length (HFSS & MDS)**
wr8-Carl

Figure 9   Im Z as a function of backshort position

At the 70 GHz fundamental frequency, the circuit impedance is purely inductive and independent of the power backshort position. However, at the 140 GHz second-harmonic frequency the impedance moves along a circle on the smith chart as the power backshort is adjusted; the impedance is plotted on a linear scale in Figures 8 and 9. Hence, with a properly designed cavity the near optimal second harmonic impedance of approximately 7+j7 ohms can be easily achieved with this cavity design. However, the TEO bandwidth is bounded at low frequency by the second-harmonic resonance condition at 108 GHz. As shown in Figure 8, the second harmonic impedance is shorted at 108 GHz and not tunable by the power backshort. Although not shown, the fundamental impedance at 54 GHz is well behaved. The resonance at 108 GHz can be moved slightly by changing the package dielectric or the width of the disc. However, changing the package dielectric only slightly effects the resonance. Increasing or decreasing the disc diameter greatly compromises the impedance transformation across the remainder of the band limiting performance at other frequencies. Therefore, the 108 GHz power dip is strongly related to l, and difficult to remove without compromising performance at other higher frequencies. The TEO bandwidth is limited at higher frequencies by the cutoff frequency of the wr8 backshort and output waveguide. Above about f1 = 73.5 GHz the fundamental power is coupled to the output and the loaded Q at f1 is greatly reduced. As described above, the magnitude of the RF voltage at f1 is greatly reduced when the fundamental is coupled to an external load or, if the resistance of the load is large enough the oscillations are terminated. Hence, the upper frequency of second harmonic operation for this wr8 cavity is about 147 GHz; at higher frequencies the output power is dominated by the fundamental frequency.

The theoretical operating point of the oscillator can be predicted by using HFSS and MDS together with the DDHB simulator. By plotting the embedding impedance for different values of l verses frequency in combination with the intrinsic diode impedance verses V_{rf1} and frequency, the operating point is defined by the points of intersection. The points of intersection are where the Kurokawa conditions hold. Figure 3, 4 demonstrate this analysis for the wr8-Carl cavity for f1 = 55-75 GHz. The operating frequency for a given l is determined by the mutual intersection of the circuit and device lines shown in figures 3a,b. For example, when l = 53.9 mils (solid line) the points of mutual intersection are approximately 61.5 GHz and Vrf = 8.75 volts. Therefore, the self-consistent analysis of HFSS, MDS, and DDHB simulation predict a second-harmonic output at 123 GHz for l = 53.9 mils. The experimentally measured oscillator operating point for this l value in the wr8-Carl cavity at 10 volts DC bias is 120 GHz. Therefore, this complex analysis is accurate to within about 3 GHz. The other operating points predicted in Figures 3, 4 are also within 2-4 GHz accurate. As described below, the power delivered to the load at each operating point is also accurately predicted. This analysis shows that the mechanical tuning of the wr8-Carl cavity can offer continuous and smooth frequency tuning over a relatively large bandwidth; the wr8-Carl TEO is expected to have at least 27.5 GHz of bandwidth from 120-147.5. However, to achieve more than 30 GHz of TEO bandwidth in this frequency regime is probably very difficult using any mechanical or electrical tuning technique. Certainly, the fixed-tune cavities

123

(non-adjustable *l*) are limited to bias tuning which is approximately 100-300 MHz/volt for these diodes.

Experimental Results and Comparisons to Theory

To confirm the inherently broad band nature of this diode (under the constraints of limited bandwidth cavities) a set of identical diodes from several fabrication batches were tested in the four cavities described above. As shown in table 1 this design is capable of broad band second-harmonic operation, and at least 55 mW at 67 GHz , 85 mW at 122 GHz, 55 mW at 140 GHz, 29 mW at 151 GHz, and 8 mW at 170 GHz.

Cavity Style	2nd Harmonic Power (mW)	Output Frequency (GHz)
wr6	8	170
wr6	6	167
wr6	29	151
wr6	49	146
wr6	55	140
wr10-wr6	42	137
wr10-wr6	65	127
wr10-wr6	85	122
wr8-Carl	30-40	120-147.5
wr8-Carl	20-25	99-105
wr10-Carl	30	93
wr10-Carl	55	67
wr10-Carl	30	63

The results in Table 1 were attained by exploring many different pin and disc diameters and back short positions in each of the four cavities. Second-harmonic operation was confirmed by directly observing the third-harmonic power at exactly 3/2 the frequency of the measured tone. If the output power was a result of fundamental operation the next higher frequency tone would be at exactly twice the frequency. These experimental results confirm the theoretic analysis described above and show that this device has at least 84.5 GHz of bandwidth. The degradation in performance near 170 GHz is thought to be primarily due to improper impedance matching. The wr6 cavity used here was designed and optimized for operation near 140 GHz, and is probably not possible of achieving the proper impedance at 170 GHz with any set of pin and disc diameters. Similarly, the low frequency measured at 63 GHz is probably not the lowest possible frequency, but was the lowest achievable with the wr10-Carl cavity and limited pin and disc diameters.

Figure 10 demonstrates that the wr8-Carl cavity has continuous operation from 99-147.5 GHz, but a major power dip between 108 and 115 GHz. Over 30 mW of power is continuously produced from 120-147.5 GHz. This behavior is fully predictable using

HFSS, MDS and DDHB simulation. Figure 11 shows the experimental and theoretical second-harmonic power for the wr8-Carl cavity at 140 GHz and 108 GHz as a function of backshort position. The output power has been simulated using the DDHB code with the embedding impedance calculated from HFSS. As expected, the output power varies with backshort position as the impedance moves around a circle on the smith chart.
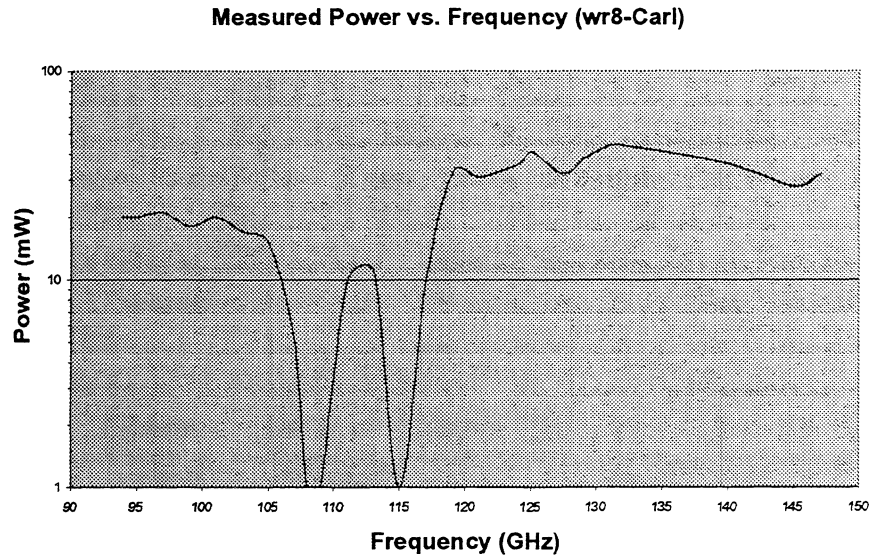
Measured Power vs. Frequency (wr8-Carl)

Figure 10   Power vs. Frequency Measured with the wr9-Carl cavity

Comparison of Figures 8 through 11 indicate the optimal impedance as well as the backshort position that essentially shorts the second-harmonic power. Reasonable amounts of second-harmonic power are generated even for backshort positions that present a capacitive load to the diode. Although the diode must be capacitive at the fundamental, at the second-harmonic the diode can appear inductive. This is a direct outcome of the nonlinearity of the device impedance which produces undriven harmonic currents and voltages with phase relationships controlled by the linear embedding impedance of the circuit. For 108 GHz the output power is very low and independent of back short position since a strong resonance occurs within the coaxial section; the device is essentially shorted at the second-harmonic.

Conclusion

We have shown experimentally that a single-style InP second-harmonic TED can produce moderate amounts of output power over the frequency range of 63-170 GHz. An accurate theoretical analysis using HFSS, MDS, and DDHB has been used to show that this device is capable of operation from 60- 200 GHz with proper cavity design. A mechanically tuned cavity is described that continuously tunes from 99-147.5 GHz with no detectable frequency jumps, and produces 30-40 mW of power over the 120-147.5

GHz band. Future experimental and theoretical investigations are focused on new diode and cavity designs capable of moderate output power (10-30 mW) in the 200-150 GHz regime.

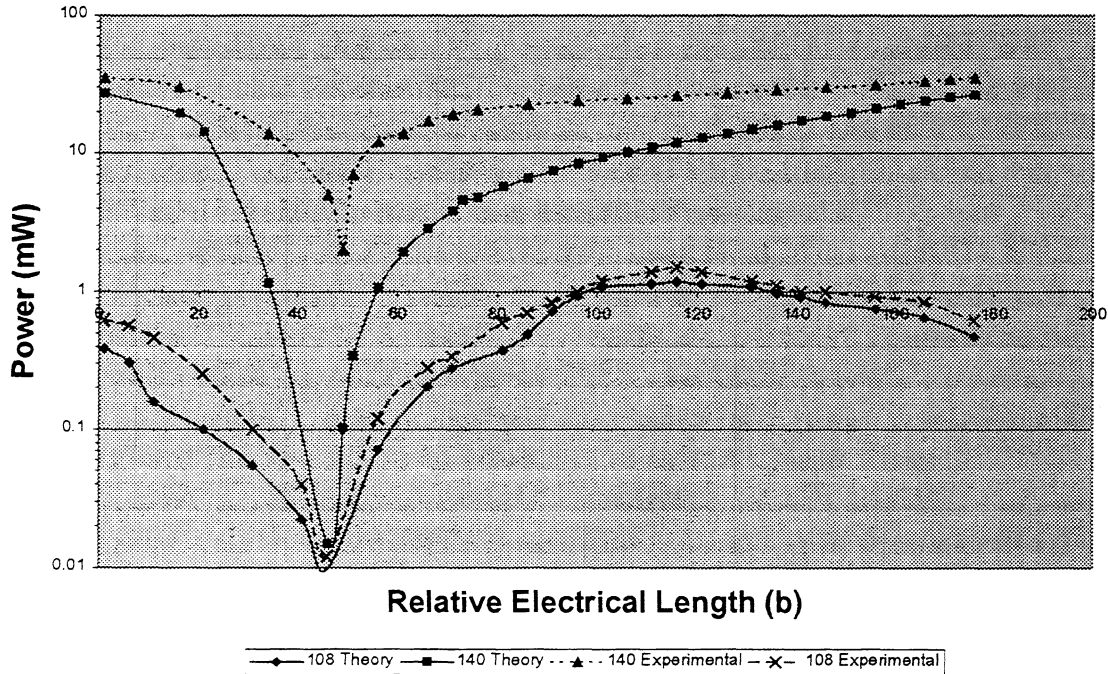**Power vs. Backshort Position (b) @ 108 GHz and 140 GHz**

Figure 11 Theoretical and Experimental power vs. backshort position for the wr8-Carl cavity

References

1. J.D. Crowley, C. Hang, R.E. Dalrymple, D.R. Tringali, F.B. Frank, L. Wandinger, B. Wallace, Electron. Lett., 30, 499 (1994).
2. M.F. Zybura, S.H. Jones, B.W. Lim, J.D. Crowley, J.E. Carlstrom, Solid State Electronics, vol. 39, No. 4, pp 547-533 (1996).
3. H. Eisle, G.I. Haddad, Proceedings of the 1995 Symposium on Space Terahertz Technology, Pasadena, CA (1995).
4. A. Rydberg, Int. J. Infrared Millimeter Waves, 11, 383, (1990).
5. J.E. Carlstrom, R.L. Plambeck, D.D. Thornton, IEEE MTT, MTT-33, No. 7, (1989).
6. M.F. Zybura, J.R. Jones, S.H. Jones, G. Tait, IEEE MTT, vol 43, No. 4, (1995).
7. G. Tait, IEEE Microwave and Guided Wave Lett., vol 4, No. 12, (1994).
8. K. Kurokawa, Bell Systems Technical Journal, (1969).